

Test of the prototype of VEPP-5 preinjector.

A.V. Aleksandrov, M.S. Avilov, A.V. Antoshin, P.A. Bak, O.Yu. Bazhenov, Yu.M. Boilmel'shtein, R.Kh. Galimov, K.V. Gubin, N.S. Dikansky, A.G. Igolkin, I.V. Kazarezov, V.E. Carlin, N.A. Kisileva, S.N. Klyushchev, O.V. Koroznikov, A.N. Kosarev, N.Kh. Kot, D.E. Kuklin, A.D. Lisitsin, P.V. Logatchev, L.A. Mironenko, A.V. Novokhatski, V.M. Pavlov, I.L. Pivovarov, A.M. Rezakov, V.S. Severilo, Yu.I. Semenov, B.A. Skarbo, A.N. Skrinsky, D.P. Sukhanov, Yu.F. Tokarev, A.V. Filippov, A.R. Frolov, V.D. Khambikov, A.N. Sharapa, A.V. Shemyakin, S.V. Shiyankov.

BINP, 630090 Novosibirsk, Russia.

Introduction.

The prototype of VEPP-5 preinjector [1,2] was created in order to perform the general tests of an accelerator elements. It represents an initial part of a preinjector and consists of (see fig.1): a 100 keV thermionic electron gun, an RF module on the basis of klystron KIU-12, a subharmonic buncher, a pulse compression system, an S-band bunching section, an accelerating section, a beam transport system and system of beam monitoring. This article presents the basic results of the prototype tests with the 2.5-meter-long accelerating section. The average accelerating rate of an electron beam up to 17 MeV/m was achieved with up to $1.2 \cdot 10^{10}$ particles per pulse accelerated. During the present experiments the subharmonic buncher is not used.

General description of the prototype.

The electron bunch produced by the 100 keV thermionic gun. The output energy of the beam from the gun is 100 keV and the length of the current pulse (FWHM) is 2.5 ns.

The continuous RF signal ($f = 51.8$ MHz, $U = 100$ mV) from master oscillator G4-164 comes through the frequency up-converter to the step controlled 180° phase shifter. Then it is amplified by the sub-klystron KIU-37 which drives the klystron KIU-12. After KIU-12 the RF pulse with length of ~ 2.5 mks transmitted to the SLED type pulse compression system. From the output of the SLED compressor the RF pulse comes to the input of the accelerating section (AS). The part of the power after SLED is coupled through the directional coupler ($\alpha_{\text{coup}} = 28$ dB) to the RF buncher.

Remotely-controlled attenuator and phase shifter is used to adjust the amplitude and the phase of RF pulse at the buncher's input.

The pulse compression system SLED consists of the 3dB coupler and two cylindrical cavities with high Q, operating in TE_{015} mode. The fine tuning of the cavities is performed by deformation of one of the cavity walls with the help of the step motor. Unloaded quality factor of the cavities $Q_0 = 10^5$, coupling factor

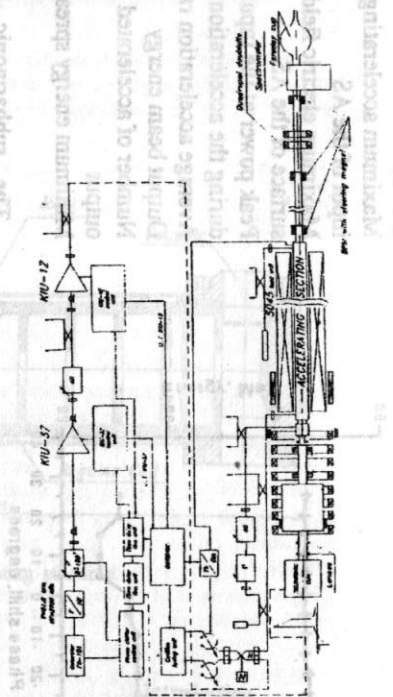


Fig. 1 The general layout of the preinjector prototype.

with a wave guide $\beta = 5.7$, unloaded time of cavity $\tau_0 = 11.9$ mks. The specific parameters of the cavities were chosen to provide the quasi constant gradient along the AS at the submission on it RF pulse after SLED system.

S-band bunching section consists of four coupled cylindrical cavities (3 cells + 1 coupler) and operates in the $\theta = -4\pi/3$ mode.

The accelerating section of the prototype is the cylindrical disk-loaded waveguide with a constant impedance with $\beta_{ph} = 1$, and phase shift per cell is $\theta = 2\pi/3$. Shunt impedance of the section is $R_{sh} = 59.3$ M Ω /m. The section consists of 68 cells and 2 couplers. Filling time of the section is $T_f = 0.441$ mks.

The beam transport system of the prototype consists of 2 magnetic lenses, 6 ring coils (diameter $d=525$ mm, operating current I up to 510 A) and a solenoid (internal diameter $d=160$ mm, external diameter $D=320$ mm, length $L=2300$ mm, operating current I up to 1100 A), quadruple doublet and steering magnets (see fig.1).

The control system can vary the operating currents either in the basic focusing system or in the steering magnets. The position of a beam is controlled by beam position monitors, located at the output of the thermionic gun and at the input and the output of the AS.

Measurements of the total charge of the bunch from the thermionic gun are produced by wall current monitor, installed before the input of the buncher (see fig. 1). The charge of the accelerated bunch after the AS is measured by the Faraday cup. The measurements of the energy characteristics of the beam are carried out by 180° spectrometer. The beam is spotted on the luminiscent screen at the spectrometer exit.

The experiments and results of the measurements.

For the effective use of the accelerating section, the beam injection (the triggering of the electron gun) should be done after complete filling of the section by an rf-pulse, i.e. in time $\tau = L/v_p$ after 180° RF phase switch. Since the filling time of the section $T_f = 0.44$ mks is comparable with time of the signals propagation in supervising and control circuits, the exact moment of the electron gun triggering was determined experimentally by the maximum output beam energy.

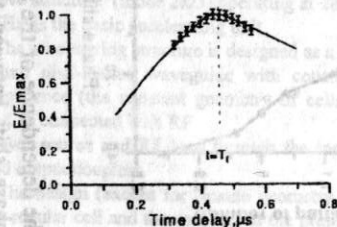


Fig. 2 The dependence of the bunch energy on time delay (solid line - theoretical calculations).

Using the measured power pulse shape at the AS

input one can determine the total beam energy gain $E(\tau)$, where τ is the moment of the electron gun triggering. Fig. 2 shows dependence $E(\tau)/E_{\text{max}}$. The dots on the diagram correspond to experimentally measured values when the optimum time delay of a current pulse of the electron gun is determined.

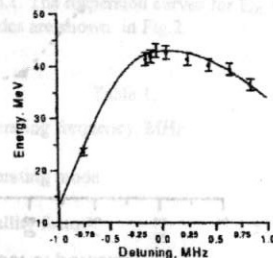


Fig. 3 The dependence of beam energy gain on the frequency detuning. Solid line is computer simulation of the beam motion, dots - experimental data.

Fig. 3 shows the maximum energy, gained by particles in the AS vs. the value of the detuning $\Delta f = f - f_0$. The dots in the plot correspond to experimentally measured energies of the electron bunch in the process of determination of the AS operating frequency. The zero value of the detuning corresponds to $f_0 = 2798.3$ MHz, at which the maximum of accelerated bunch output energy is reached.

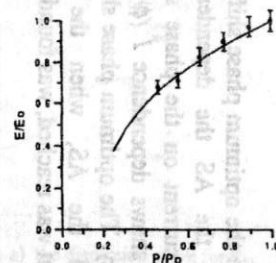


Fig. 4 The dependence of relative output energy of the bunch on input power P/P_0 at the operating frequency of the AS. Dots correspond to measured values of the maximum output bunch energy.

Fig. 4 shows the dependence of the relative maximum output energy of the bunch on the input power P/P_0 at the operating frequency of the AS. Dots correspond to measured values of the maximum output bunch energy.

In order to choose the optimum phase shift ϕ between the buncher and the AS the dependence of the accelerated beam current on the phase shift ϕ was measured. Fig. 5 shows dependence $I(\phi)$ at the AS operating frequency. The optimum phase shift between the buncher and the AS, when the maximum accelerating current was reached, was found.

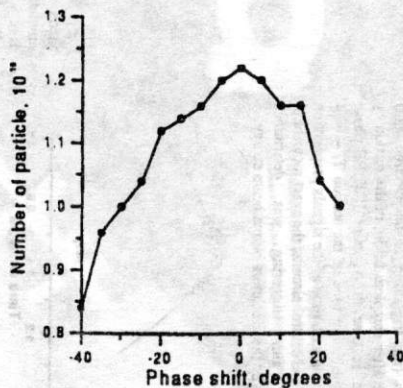


Fig. 5 The dependence of the accelerated beam current on the phase shift between the buncher and the AS (experimental data).

Fig. 6 shows the dependencies of the accelerated beam energy and energy spread in the bunch on the phase shift between the buncher and the AS.

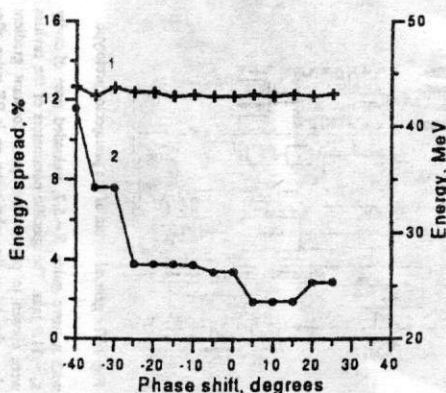


Fig. 6: The dependence of the accelerated beam energy (curve 1) and energy spread (curve 2) on the phase shift between the buncher and the AS.

It is obvious, that the minimum energy spread in the bunch is also reached near the chosen zero of the phase shift, and there is rather weak dependence of the beam energy on the phase shift between the buncher and the AS.

Besides this, to check the efficiency of the buncher operation, the dependence of the beam current on the RF power at the input of the buncher $I(P_{gr})$ was taken. In that case the RF-power at the AS input remained constant. This dependence is presented in fig. 7.

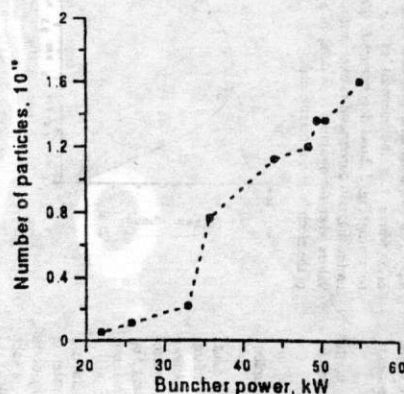


Fig. 7 The dependence of the beam current on the RF power, at the input of the buncher.

Rather strong dependence of the beam current intensity on the field in the buncher is clearly seen, that confirms efficiency of bunching.

The experiments on the prototype were started in October 1996. The most important parameters of the prototype achieved in operation are:

Repetition rate	50 Hz
Number of particles in the bunch	$5 \cdot 10^{10}$
Operating frequency of the AS	2798.3 MHz
Maximum peak power at the input of the AS	46.4 MW
Maximum accelerating field at the input of the AS	24.5 MV/m
Maximum electric field on the surface of the AS	49 MV/m
Peak power at the input of the AS during the acceleration	28.5 MW
Average acceleration rate	17.7 MeV/m
Output beam energy	44.3 MeV
Number of accelerated particles at the output	$1.2 \cdot 10^{10}$
Minimum energy spread in the bunch	$\pm 1\%$

The subharmonic buncher, operating on 16-th subharmonic of basic frequency (174.8 MHz) is preparing for RF tests. It's successful operation will permit to check up the performance of the initial part of the preinjector in a single bunch mode.

References.

- [1] A.V. Aleksandrov et al., "Preinjector for electron-positron factories". Proc. 1994 XIV Conf. On Charge Part. Acc., Protvino, Russia.
- [2] A.V. Aleksandrov et al., "Electron-positron preinjector of VEPP-5 complex". Proc. 1996 of the XVIII Int. Linear Acc. Geneva, Switzerland. Pp. 821-823.

THE ACCELERATING STRUCTURE FOR VEPP-5 PREINJECTOR

A.N. Kosarev, D.E. Kuklin, A.V. Novokhatski, V.V. Podlevskih, S.V. Shiyankov.

Budker INP, 630090 Novosibirsk, Russia.

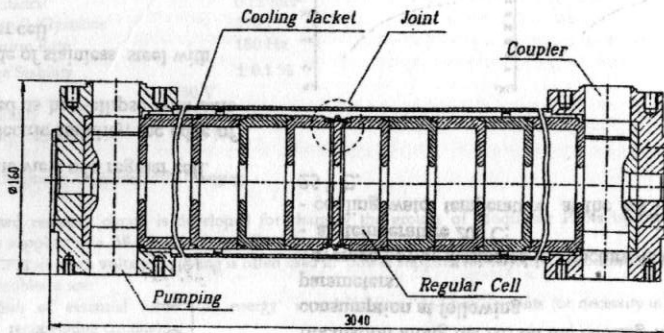


Fig. 1 The accelerating structure.

Abstract

At present time in the Budker INP the serial production of the accelerating sections (AS) for VEPP-5 preinjector has begun.

In this paper the electrical engineering parameters of the AS are presented. The separate elements of the construction and technology of the AS production are described.

Introduction

According to the preinjector project the basic requirements to the AS were determined as:

a) the efficiency of the input RF pulse energy use in the assumption of AS excitation by the KLYSTRON 5045 with the SLED-type power compression system;

b) the high electrical performance of the system;

c) the relative technological simplicity of the production of either the separate elements or the whole structure when the tough requirements to the tolerances are maintained;

d) the high reliability of the system.

After the comprehensive study the prototype of the AS was produced.

The following technological problems were solved during the AS prototype production:

- the development of the technology of the most complicated AS elements: the coupler, the transitive assembly etc.;
- the reliable vacuum connection of all elements of the structure with full electric contact;
- the maintenance of all technological tolerances and high quality surface of the AS elements.

THE ACCELERATING STRUCTURE

We suggest to use an accelerating travelling wave structure (mode $2\pi/3$) operating at 2856 MHz as the basic accelerating unit.

The accelerating structure is designed as a round disk-loaded waveguide with constant impedance (the constant geometry of cells) and is connected with RF power source and RF load through the input and output couplers.

The design (except for inside geometry of the regular cell and the coupler) of the present accelerating structure totally corresponds to that of the AS for VEPP-5 preinjector prototype (operating frequency 2798 MHz), which is constructed and tested at the INP in

1996 with the accelerated electron beam obtained.

The general layout of the AS is shown in Fig. 1. The AS parameters are presented in Tab. 1. The dispersion curves for E_{01} and EH_{11} modes are shown in Fig. 2.

Table 1.

Operating frequency, MHz	2856
Operating mode	$2\pi/3$
Quality factor	$1.32 \cdot 10^4$
Group velocity, c	0.021
Shunt impedance, MOhm/m	51
Surface field enhancement	2.02
Number of cells	85
Length of the section, m	2.93
Filling time, μ s	0.471

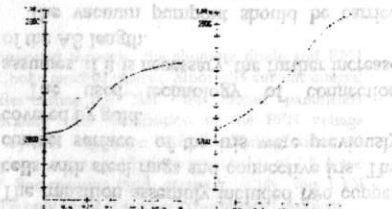


Fig. 2 a) the dispersion curve for E_{01} mode;

b) the dispersion curve for EH_{11} mode.

Fig. 2 shows the schematic view of a regular cell, and geometrical parameters of it are presented in Tab. 2.

Table 2.

Aperture diameter 2a, mm	25.90
Waveguide diameter 2b, mm	83.75
Iris wall thickness t, mm	6.00
Cell length D, mm	34.98

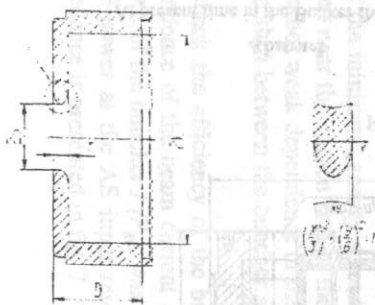


Fig. 3 Schematic view of a regular cell.

To improve the electric stability, the edge of the iris is performed as half-ellipse with axis ratio 2:1.

The coupler is made of stainless steel with the brazed-in copper cell.

The sketch of the coupler is shown in Fig.4.

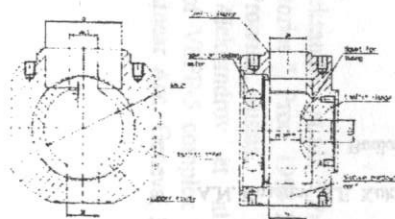


Fig. 4 The coupler

The coupler is made of stainless steel with the brazed-in copper cell.

The used design of the coupler allows to combine the following functions:

- matching device;
- vacuum pumpout port;
- cooling water input/output port.

The vacuum pumpout port is located in front of the input waveguide port. It allows to decrease the field amplitude assymetry at 10 mm from the axis down to 0.01 mm^{-1} . The cooling jacket is intended to reject the RF power dissipated in the structure and is performed as a steel pipe with the uniform cross-section. The space between the jacket and external surface of cells is 4 mm. Fig.5 shows the dependencies of the average temperature and maximum temperature fluctuation along the AS on the cooling water consumption at following parameters:

- average power dissipated in structure 4kW;
- air temperature 20°C ;
- cooling water temperature at the AS input 25°C .

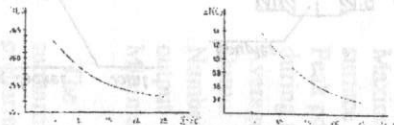


Fig. 5 The dependencies of the average temperature and maximum fluctuation along the AS on the cooling water consumption.

In addition, the cooling jacket protects the copper cells from mechanical deformation and possible deviation from the axis.

The inside geometry tolerances are primary determined by their influence to the wave phase velocity and the cost of cells fabrication. As the result, the following tolerances were admitted:
 $\Delta 2b = \pm 0.01 \text{ mm}$, $\Delta 2a = \pm 0.01 \text{ mm}$,
 $\Delta 2t = \pm 0.01 \text{ mm}$, $\Delta 2D = \pm 0.02 \text{ mm}$.

Follow these tolerances one can provide rms phase velocity deviation along the structure not more than 0.3%.

M0b copper was used for the AS cells fabrication. The fabricatin process included the cold pressing under the 1500 kg/cm^2 in a special appliance, anneal and following turning of the cells with the diamond tool.

The used technology provided the high precision of all tolerances maintenance (the defective cells are not exceeded 2% from the total production).

The tolerance control was carried out by the result of RF measurements of cells.

The surface control was carried out by interference method and showed that used technology provides $R_a \leq 0.025 \mu\text{m}$.

The AS brazing is one of the most complicated technological operations which is carried out in the furnace in a specially produced appliance.

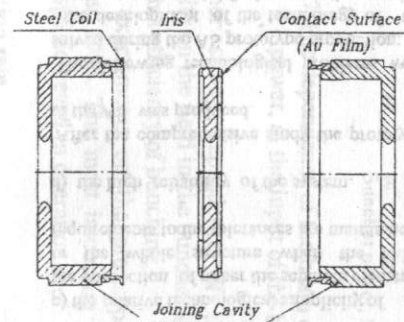


Fig. 6: Transitive assembly.

The developed construction of the connection device and the used technology of brazing provided the high reliability of all brazed connections, full electric contact and allowed to avoid the gaps and leakage of the brazing alloy inside the structure.

The process of the AS production consists of two half-structures brazing and their connection through the transitive assembly. The transition assembly included two copper cells with steel rings and connective iris. The contact surface of the iris were previously covered by gold.

The used technology of connection assumes, if it is necessary, the further increase of the AS length.

The vacuum pumpout should be carried out simultaneously through the both couplers and provides the vacuum not worse than 10^{-8} Torr along the structure.

At present time in the INP workshops the serial production of 14 AS for VEPP-5 preinjector has begun.

References

- [1] A.V.Aleksandrov et al., "Test of the prototype of VEPP-5 preinjector", INP 97-64, Novosibirsk, 1997.

The Resonant "de-Tailing" Stabilized Charging System

for High Power Klystron Modulators

A. S. Medvedko, S. P. Petrom

1.0. Introduction.

The important goal in development of the Klystron power supply for the Next Linear Collider (SLAC Project) is attaining of maximum efficiency and reliability of the system requirements of under the Klystron technical Specification. This is determined by the large number of Modulators and Klystrons.

The large total power of the power supply system requires also the uniform load distribution over phases of the mains with its moderate distortions.

This report describes the possible variant of the Power Supply system that may be proposed for charging the Modulator Pulse-Forming Network (PFN).

1.1. The Parameters of Power Supply Source for Charging the Modulator PFN Capacitors (2 Klystrons are supplied by one Modulator) [1].

PFN Voltage	72 kV
PFN Capacitance	0.12 mF
Joules / pulse, 2 Klystrons	310 J
Pulse Repetition Rate	180 Hz
PFN Voltage Stability	± 0.1 %
AC Line	480 V
AC Line Stability	3 %
Power Supply Efficiency	> 93 %

2.0. Suggested Circuit Diagram of Modulator PFN Charging.

The proposed resonant circuit is developed for charging the groups of Modulator PFNs by the charging circuits that supplied by a 38-40 kV nonstabilized power rectifier.

A resonant circuits with voltage doubling is often used in power supplies for Klystron's Modulators [1,2]. But serious problems are:

1. Dissipation of essential value of energy in stabilization "de-Qing" circuits (or necessity in designing of special recuperating circuits).
2. Providing of uniform loading of AC mains (especially when total power is of considerable value).

The proposed circuit enables the uniform distribution of the load as Modulator groups with working frequencies 60, 90, 120, 180 Hz. In order to have a possibility to distribute uniformly the load over the mains phases at these frequencies the number of Modulators supplied by one power rectifier should be either 12 or 24 (or to be a multiple).

The stabilization of the PFN capacitors voltage is achieved by cutting OFF of the "Tail" of resonant process of capacitors charging. This approach to a question of voltage stabilization can be named as "de-Tailing" method. With using of this method no additional energy (beside ordinary losses in switches and resistors) dissipates in charging circuit during stabilization process. It allows us to design charging system with maximum value of power efficiency.

2.1. Functional Circuit Diagram of Charging System.

The General Circuit Diagram consist of common DC PS (rectifier) and 12 (24) resonant cells. For one cell Diagram is presented at Fig. 1.

The DC Power Supply Source is a 6-phase Bridge Rectifier with an output voltage of 38-40 kV.

For each individual modulator the power supply cell consist of the ON/OFF controlled Switch with a protective Diode commutating current up to 5 A at voltage of 38-40 kV, the charging Choke with an inductance of approximately 6 H with maximum current up to 5 A, a Shunting Diode behind the Switch ant Cut-off Diode in series with charging Choke. Capacitors C_{PFN} presents the equivalent capacitance of PFN, operating on the load (Klystrons) through Thyatron.

The rated input transformer and rectifier power is about 0.7 MW when feeding 12 Modulators with the repetition rate of 180 Hz and its power is 1.4 MW when feeding 24 Modulators. The version of separate supplying of Modulators with the use of individual power transformers and rectifiers is also possible but in this case, however, the power supply system efficiency is substantially reduced.

The primary voltage of rectifier transformer can be arbitrary ranging from 480 V to 110 kV and it is to be selected depending on conditions of mains distributing system. Primary mains voltage of 15 to 35 kV (line) is preferable because of fewer quantity of transformer stages at distribution system, availability of convenient commutation devices and small losses in distribution wires.

2.2. Operation of Power Supply System.

A 6-phase rectifier with an output voltage of 38-40 kV provides the DC power during the charging of the PFN. In the beginning of every 1/6 period of the mains Line (60 Hz) the Switch energizes the appropriate resonant circuit consisting of a Choke and 0.12 mF capacitance of PFN. The charging process is presented at the Fig. 2. Upon passing some integral of current through charging Choke the Switch is forced to be switched OFF and cuts the "Tail" of current in charging process. The "de-Tailing" process is shown in Fig. 3

After one half of period of the resonant process i.e. in 2.4-2.7 ms the capacitors have been charged up to voltage of 72 kV, the Cut-off Diode disconnects the PFN from the rectifier, and in the beginning of a next 1/6 fraction of AC period the process is repeated for the another group of charging cells.

The grouping of charging cells by 12, 8, 6, 4 for every 1/6 part of AC mains voltage enables the operation with frequencies 180, 120, 90, 60 Hz, respectively with the uniform load of feeding mains voltage. The kind of grouping and repetition frequency rate are readjusted by the control and synchronization circuits without commutations in power circuits.

2.2.1. Stabilization of PFN Voltage.

During "de-Tailing" time the charging circuit is connected through the shunting diode and PFN capacitors voltage increases on the value determined by the Choke residual current. Since the current integral can be found with quite high accuracy and in time left after cutting the "Tail" the circuit parameters (inductance, capacitance, resistance) cannot change significantly the stabilization of the PFN voltage capacitance can be achieved on the required level 0.1 % by the regulation of "de-Tailing" time. As calculations have shown, when cutting the "Tail" of charging process at Choke current value of 1.8 A the voltage on the PFN capacitors increases from 71 to 72 kV. For ensuring total accuracy 0.1% this 1 kV additional voltage must be determined with accuracy about 10% only and it is not very complicated problem.

We can compare the residual value of energy stored in charging Choke with energy necessary for charging of PFN capacity from voltage $U(t)$ after "de-Tailing" up to nominal value U_{nom} :

$$L \cdot I_{ch}(t)^2 / 2 = C (U_{nom}^2 - U(t)^2) / 2$$

At the moment, when this equation will be fulfilled the Switch must be switched OFF and PFN capacitors will be upcharged precisely to nominal voltage 72 kV.

PFN voltage and Choke current measurements and necessary processing of these data can be carried out by both analog and/or digital devices. Here it is shown only one of possible methods of PFN voltage stabilization. The consideration of this problems is not the task of present report.

3.0. System Components.

The basic components of charging system of Klystron Modulator PFN are the diode (thyristor) Rectifier with power Transformer, commutating Switch Shunted with a protective Diode, charging Choke, Shunting and Cut-off Diodes.

3.1. Rectifier.

As already mentioned above, it is advantageous to use one power supply for the groups of Modulators with individual charging circuits, for example, by 12 or 24 Modulators in a group. It is also economically beneficial to provide the transformer primary voltage within the range of 15 to 35 kV. Although, the low primary voltage (from 480 V) is also possible under special requirements but the efficiency will be worse. The rectifier power is of 0.7/1.4 MW. The nominal rectifier output voltage is 38-40 kV. The output current is 18 A for 12 cells (0.7 MW) and 36 A for 24 cells (1.4 MW).

The rectifier voltage is not regulated but to provide the slow switching ON and fast switching OFF of the system (in the case of hazard) it is reasonable to make rectifier bridge with thyristors.

The computer simulated values of voltage and current in the AC mains Line with the delta/star connection of transformer's windings are shown in Fig. 4.

The power transformer should be manufactured in the oil cooling variant. In this case, the version with location of power rectifier in the transformer tank is possible.

With the rectified voltage 38-40 kV the rectifier bridge arm can be assembled with 25 thyristors of 2 to 3 kV nominal voltage (this quantity can be smaller with using thyristors of higher nominal voltage). At the voltage drop on every open thyristor of 2 V and an average value of charging cell consumed current of 1.5 A the power dissipated in the rectifier is 150 W per one modulator.

3.2. ON/OFF controlled Switch.

The Switch provides the energizing of PFN charging system and regulation of PFN capacitors voltage by cutting off the "Tail" of charging process in the moment required (de-Tailing). The Switch voltage of the OFF state does not exceed 40 kV. The current amplitude is 5 A for the ON state, the average current value is of 1.5 A.

At the role of basic elements of the Switch it can be used bipolar transistors, IGBT transistors, Gate Turn-Off thyristors. For reverse voltage elimination the reverse Diode in parallel to transistor Switch is needed. For example we consider the Switch assembled of 30 IGBT transistors (as more convenient in operation) with nominal voltage 1.7-2 kV. At 3V voltage drop for the ON state on every transistor and 180 Hz operating frequency the power of 150 W will be dissipated in the Switch. The commutation losses is negligible since the energizing is made at zero current in the circuit with high inductance and deenergizing occurs with a current not exceeding 0.5 of the maximum charging current, i.e. up to 2.5 A but with the low frequency of 180 Hz. The protective Diode does not dissipate any energy.

The diving and gate supplying circuits can be made with optical link or with transformer coupled link depending on some additional conditions.

3.3. Charging Choke.

For providing time of half-period of charging process 2.4-2.7 ms (Duration of 1/6 AC voltage period is 2.77 ms) the Choke inductance should be 6 H (PFN capacitance is 0.12 mCf).

The voltage maximum value on the Choke does not exceed 40 kV.

The Choke is estimated to be made with transformer steel core. The core cross-section is about 0.005 m². The total nonmagnetic (and insulation) gap is 50 mm. The number of turns in the winding is 6000 made of copper wire of 1-1.2 mm² cross-section. The winding is divided into 10 sections by 600 turns each with the core part in each section. The insulation layings providing both the electric insulation and nonmagnetic gap are placed between sections. The maximum core induction does not exceed 1 T. Estimated weight of Choke active part is about 60 kg. If it will be used backward magnetized core (with permanent magnet insertions) maximum induction may be up to 2 T and Choke should be smaller.

At the Choke coil active resistance of 50 Ohm and modulator operation frequency of 180 Hz the active losses in the coil are 320 W. The choke core power losses are about 50 W if transformer steel with specific losses of 1.5 W/kg will be used. Therefore full Choke losses are 370 W. This corresponds to the Quality factor of the Choke like 120, that is feasible value.

The Choke draft drawing is given in Fig. 5.

3.4. Shunting and Cut-off Diodes.

Two Diodes strings are used in the charging cell, namely, the Shunting Diode providing current circuit of charging choke after disconnecting of Switch and Cut-off Diode which cut off the PFN after its complete charging.

The Shunting Diode string maximum voltage is 40 kV and its maximum current does not exceed 2.5 A, average current is 0.1 A. If the Shunting Diode consist of 30 diodes with the voltage drop of 1.5 V for each diode, the power losses at 180 Hz frequency is 5 W.

The maximum voltage on the Cut-off Diode string is 75 kV (with the PFN charged and power rectifier off). The current amplitude value is 5 A and average current is 1.55 A. When Cut-off Diode consist of 50 diodes with the direct voltage drop of 1.5 V on each, the power losses at frequency 180 Hz is 120 W.

In addition, we will note that to use of the avalanche-type of diodes in all Diode strings are preferable because no voltage distributing resistors and capacitors necessary.

4.0. Total Losses in Charging System of PFN.

For one charging cell the losses (without power transformer) is:

Transistor Switch	150 W
Charging Choke	370 W
Shunting Diode	5 W
Cut-off Diode	120 W
Power Rectifier	150 W

Total losses in basic components are 800 W. At the full value of power for one charging cell about 56 kW the calculated efficiency is 98.5 %. Here are not taken into account losses in power transformer because of this losses depend on special data, i.e. primary AC voltage, accepted power range and so on. Usually, the transformers of these class (15 to 35 kV, 0.7 MW) have the efficiency of 98 to 99 %).

5.0. Conclusion.

One can see from all of this information that:

1. Proposed here resonant charging circuit with using of the loss-free "de-Tailing" method for voltage regulation allow to design the system for charging Klystron Modulator's PFN capacitors with extremely high efficiency and with needed accuracy.
2. For realization of "de-Tailing" method the high voltage ON/OFF controlled Switch must be designed.
3. High voltage mains with voltage range of 15 to 35 kV is to be more preferable for reducing of the cost of the system and increasing of it's efficiency.
4. Multiple number of charging cells supplied by one transformer/rectifier with rated power of 1.4 (or more) MW is favorable for AC mains uniform loading and higher efficiency of full system.

The investigation of all of these problems have especially importance for design of so large power system, as NLC Modulator PFN Charging Power System.

6.0. References.

- [1] The NLC Design Group: "Zeroth-Order Design Report for the Next Linear Collider", SLAC - 474, 1996
- [2] M.Akemoto and S.Takeda. "Pulse Modulator for 85 MW Klystron in ATF Linac", KEK Preprint 94-128, October 1994.



993